High-frequency *Wus2*-integrated transformation toolkit enhances *Cas9* editing efficiency and expands capability with *SpRY* in sorghum

Jianqiang Shen[1,3,4], Kiflom Aregawi[1,3], Sultana Anwar[1], Tamara Miller[1], Peggy G. Lemaux[1,2,4]

[1]Department of Plant and Microbial Biology, University of California, Berkeley CA 94720, USA.

[2] Innovative Genomics Institute, University of California, Berkeley CA 94720, USA.

[3] These two authors contributed equally.

[4] Correspondence Email: shenjq@berkeley.edu or lemauxpg@berkeley.edu

Abstract

Sorghum bicolor L. (Moench) ranks as the fifth most important crop globally, serving diverse purposes such as forage, food, feed, and fuel. Its natural tolerance to various environmental stresses makes it a valuable resource for addressing climate resilience. Harnessing such genetic resources for crop improvement requires highly efficient genetic transformation and genome editing tools. However, sorghum has historically been recalcitrant to genetic transformation, and publicly available engineering tools remain limited. In this study, we report a high-efficiency engineering toolkit, including shuttle and binary vectors, optimized for genome editing via *Agrobacterium*-mediated transformation. Using this toolkit, we successfully introduced CRISPR/Cas9-based editing machinery to target the *phytoene desaturase* (*PDS*) gene, achieving editing efficiencies up to 95.7% with monocistronic gRNA expression cassettes. To further expand the genome editing repertoire, we employed a protospacer adjacent motif (PAM)-flexible *Cas9* variant, *SpRY* (*ZmSpRYi*), and achieved comparable editing efficiencies. Using our toolkit increases the potential for advanced editing tools to be used in engineering genetic variation of agronomically important quantitative traits. It also paves the way for deploying advanced genome editors, such as prime editors and base editors, to manipulate genetic and genomic resources. These advances provide a robust approach for advancing research in sorghum and other cereals, offering new opportunities for sustainable crop improvement.

27 # Keywords

28 *Sorghum bicolor, Wuschel2*, transformation, editing, CRISPR, SpRY

29 # Introduction

30 Meeting future demands for crop production with more variable climate conditions and an increasing
31 world population will require growing more food and feed on less land. *Sorghum bicolor* L. (Monech) is an
32 ideal crop for future applications because of the diversity of modern germplasm, particularly with respect
33 to its multiple abiotic stress tolerances (Dahlberg, Burke, and Rosenow 2004; Paterson et al. 2009;
34 Varoquaux et al. 2019). Breeding improved sorghum varieties using targeted genome editing and marker-
35 assisted selection will accelerate development of improved cultivars (Ramstein, Jensen, and Buckler 2019;
36 Schindele, Dorn, and Puchta 2020; Zhu, Li, and Gao 2020). However, utilizing CRISPR/*Cas9* genome editing
37 in sorghum lags in efficiency relative to other crops due to low editing efficiencies, a lack of efficient
38 transformation systems for diverse genotypes, and a lack of optimized, publicly available tools. The
39 current work seeks to address all three limitations by introducing a novel set of resources for high
40 throughput sorghum transformation and genome editing.

41 Sorghum genome engineering has historically been a challenging process due to recalcitrance of most
42 sorghum genotypes to *in vitro* tissue culture and a lack of technical expertise and effective tools for
43 transformation (Altpeter et al. 2016). A significant challenge of genome engineering in crop species is the
44 requirement for germline transmission of mutations necessitating gene delivery in pluripotent cells.
45 Transcription factors, such as Babyboom (BBM) and/or Wuschel2 (WUS2), increase the population of cells
46 in target tissues that are competent for germline transmission (Lowe et al. 2016), (Lowe et al. 2018).
47 Previously we demonstrated that incorporation of transient *Bbm* and *Wus2* expression during sorghum
48 Agrobacterium-mediated gene delivery increases transformation frequency for several recalcitrant
49 varieties (Aregawi et al. 2022). Concurrently, Che et al. demonstrated that during sorghum transformation
50 incorporation of the *Wus2* morphogenic gene alone increased CRISPR/*Cas9*-mediated gene dropout rate
51 of the *Brown midrib* gene (Che et al. 2022). The breakthrough in transformation technology due to
52 morphogene-assisted transformation has greatly expanded the possibility of genotype-independent gene
53 editing; however, developing tools for high efficiency genome editing with CRISPR remains a challenge.

54 The CRISPR/*Cas9* genome editing system**,** first discovered as a component of the adaptive immune
55 response in *Streptococcus pyogenes* bacteria (Jinek et al. 2012), is a powerful tool for genome editing that
56 has potential for functional genomics and accelerated breeding in plants (Zhang et al. 2019). Editing in
57 non-model plants lags in efficiency compared to animal and bacterial systems, due to several factors,
58 including the plant 'regeneration bottleneck' and sub-optimal *in planta* expression of editors.
59 Optimization of the Cas endonuclease, guide RNA expression and use of Cas variants with expanded PAM
60 recognition sequences have been proposed to increase the efficiency of gene editing in plants (Liu, Li, and
61 Godwin 2019; Q. Ren et al. 2021; Xu et al. 2021). To overcome these challenges, codon optimization of
62 the Cas9 nuclease was used to increase gene knockout editing efficiency in Arabidopsis and tobacco
63 (Castel et al. 2019; Grützner et al. 2021). The use of specific promoters and guide RNA transcriptional
64 configurations has been shown to increase sorghum editing efficiency as demonstrated when using the
65 endogenous U6 promoter driving gRNAs (Massel et al. 2022). Another inherent limitation to the capacity
66 for introducing genetic variation at specific sites is the fact that the canonical *Cas9* endonuclease requires
67 the NGG (N = A, T, C, and G) Protospacer Adjacent Motifs (PAMs) site, which severely limits the genome
68 sites available for editing. Several Cas variants have been engineered to overcome the PAM limitation of
69 *SpCas9* (Tang et al. 2017; B. Ren et al. 2019; Ming et al. 2020). *SpRY* endonuclease is an engineered variant
70 of *Streptococcus pyogenes Cas9* with a nearly PAM-less requirement and has been used for base editing
71 and functional genetics in rice (B. Ren et al. 2019; Q. Ren et al. 2021; Xu et al. 2021).

72 The present work addresses three main goals for advancing transformation and editing of complex traits
73 in *Sorghum bicolor*: increasing the efficiency of CRISPR/*Cas9* editing, expanding available PAM recognition
74 sites, using the Cas9 variant, ZmSpRYi and providing needed genome editing capability to public
75 researchers. We developed a flexible functional genomics toolbox for Agrobacterium-mediated sorghum
76 transformation and genome editing. The toolbox includes a binary T-DNA vector incorporating the *Wus2*
77 gene, along with *hygromycin B phosphotransferase* (*hph*) and *ZsGreen* (*ZsG*) as selection and visual
78 markers. For CRISPR/*Cas9* genome editing, we utilized an intronized Cas9 endonuclease in a shuttle
79 vector, enabling easy insertion of designed guide RNA sequences. Additionally, for the first time in
80 sorghum, we demonstrate editing with the nearly PAM-less Cas9 variant ZmSpRYi, employing mono- or
81 poly-cistronic guide RNA expression. Overall, this high-efficiency toolbox enhances the scalability of
82 genome editing in sorghum, enabling faster breeding and supporting advancements in synthetic biology.

Results

Design of high efficiency binary and shuttle vectors

A two-step strategy was developed that involves gRNA validation in protoplasts, followed by stable plant genetic transformation (**Figure 1A**), that enhances efficiency and accessibility for researchers to perform sorghum transformation and editing. The editing machinery is integrated in a Level 1 construct, the shuttle vector, which facilitates guide RNA (gRNA) customization through insertion of either polycistronic or monocistronic transcriptional units (**Figure 1B**). The gRNA scaffold and Pol III promoters necessary for driving gRNA expression are supplied by the Level 0 constructs (**Figure S1**). These two elements are sequentially assembled to form complete gRNA transcription units, which are transfected into sorghum protoplasts to evaluate editing efficiency of the gRNAs (Jores et al. 2021; Lee et al. 2023).

To enhance efficiency of sorghum transformation, a series of binary constructs were developed, all of which are compatible with Gateway LR recombination and tailored to incorporate genes of interest for multiple applications (**Figure 1C**). The foundational construct, pGL206, includes a *hygro*mycin resistance gene (*hph*) as a selectable marker (**Figure 1C**). Hygromycin was chosen for its stringent selection properties during in vitro tissue culture of sorghum (van den Elzen et al. 1985). This construct serves as a platform for testing candidate morphogenic genes, i.e., maize *Wuschel2* (*Wus2*). To facilitate tracking of somatic embryogenesis and plantlet development, a visible marker *ZsGreen1,* driven by the sorghum ubiquitin promoter, was incorporated near the T-DNA left border; this construct is pGL216. Building on previous findings of enhanced editing efficiency with integration of maize *Wus2* (Che et al. 2022), the construct, pGL216, was assembled with *Wus2*, driven by the maize phospholipid transfer protein promoter (PLTP) (**Figure 1C**). This modification led to development of pGL222 (**Figure 1C**), a binary vector optimized for delivering genome-editing machinery. Presence of the fluorescence marker validates the presence of at least one complete T-DNA copy and easy visualization of T-DNA segregation in the T_1 generation. These constructs provide a robust framework for improving transformation and genome-editing efficiencies in sorghum.

Transformation and editing frequency using *Wuschel2* integration

To evaluate transformation frequency in genome editing trials, we targeted the *Sorghum bicolor phytoene desaturase* (*SbPDS*) gene using two gRNAs, PDS gRNA1.1 and 2.2 (**Figure 3A**), designed to knock out its function (Aregawi et al. 2022). Previous studies in wheat and Setaria indicated editing efficiency may vary depending on the nature of the transcriptional units of gRNAs in C3 and C4 grasses (Liang et al. 2021; Milner et al. 2024); however, this has not been thoroughly investigated in sorghum using CRISPR/*Cas9*. To study this, constructs were designed containing two gRNAs under two transcriptional configurations, polycistronic and monocistronic (**Figure 1B**). In the first construct, gRNAs were expressed from a polycistronic unit, driven by the sorghum snoRNA U6.2.3 promoter (Massel et al. 2022). In the second, gRNAs were expressed in separate monocistronic units driven by the snoRNA U6.2.3 and snoRNA U6.3.1 promoters (Massel et al. 2022). Both validated gRNA transcriptional units were combined with a Cas9 expression cassette and integrated into the binary vector pGL222, resulting in two editing constructs, pGL221 (polycistronic) and pGL220 (monocistronic) (**Figure S2**). These constructs, containing the morphogenic gene *Wuschel2* (*wus2*) and the selectable marker gene, *hph*, were used to assess the impact of gRNA transcriptional configurations on editing efficiency.

These two constructs were transformed into sorghum immature embryos (IEs) using a modified protocol (Aregawi et al. 2022). In this approach, the heat treatment typically applied after the callus resting stage was omitted, because the *Wus2* expression cassette was not excised after integration (**Figure 2A**). Following Agrobacterium infection, the IEs were maintained at 25°C for one week on co-cultivation media. Previous studies indicated that higher temperatures may enhance mutagenesis efficiency when employing CRISPR/*Cas9* in plants (Milner et al. 2020; Blomme et al. 2022). To explore this, tissues were incubated at either 25°C or 28°C until plant regeneration. Development of IEs were monitored to evaluate their responses to *Wus2* expression at 1-, 2-, and 4-weeks post-infection (**Figures 2B–E**). Fluorescence signaling was detected as early as one week after infection (**Figure 2B**) and peaked at the end of the resting stage (**Figure 2C**). Somatic embryogenesis was most prominent during the two-week time period, with regenerated plantlets forming by the fourth week (**Figures 2D–E**). Prior to transferring the putative regenerants to rooting media, fluorescence microscopy was used to screen for ZsGreen expression, confirming integration of the full-length T-DNA, given that the ZsGreen expression cassette is located adjacent to the right border. Subsequently, putative transgenic plantlets were analyzed via PCR to further confirm T-DNA integration.

140

141 Transformation and editing efficiencies were calculated using two strategies. The first was calculated
142 when including only one transgenic plant from each IE, the second when including all regenerated
143 transgenic plants. Each way has its advantages. Considering a single plant per IE is helpful when using
144 overexpression to get independent transgenic plants. Unlike when using a classical sorghum
145 transformation strategy, here we regenerated multiple plantlets from each IE. Transformation frequency
146 indicates the proportion of IEs within the total IEs used that successfully produce transformants.
147 Regarding the editing events, considering all regenerants derived from a single IE is beneficial as multiple
148 independently edited events can originate from the same IE.

149

150 When considering only one plant per IE at 28°C for the monocistronic strategy, we generated 50
151 transgenic plants from two replicates, giving a transformation frequency of 24.4%. Given 79
152 transformants, an average transformation frequency of 36.6% was obtained from the polycistronic
153 strategy. Unlike the 28°C result, tissues incubated at 25°C showed normal phenotype. Because of this
154 difference, more plants were regenerated, increasing the transformation frequency to 31.4% and 43.3%
155 for the monocistronic versus polycistronic strategies, respectively.

156

157 When all regenerated transgenic plants were considered, transformation frequency substantially
158 increased (**Table 2**). At 25°C, the monocistronic and polycistronic strategies yielded transformation
159 efficiencies of 82.9% and 100%, respectively. At 28°C, the monocistronic and polycistronic strategies led
160 to 66.9% and 62.7% transformation efficiencies, respectively. In general, tissues kept at 28°C showed more
161 necrosis than those kept at 25°C (**Figure S3**). This reduced the number of regenerated plants and thus the
162 transformation efficiencies were lower (**Table 1**).

163 Wuschel-mediated CRISPR/*Cas9* editing and editing efficiency

164 Previous work demonstrated that various factors are needed to improve CRISPR/*Cas9* editing efficiency.
165 One factor is intronized and maize codon-optimized *Cas9* (Castel et al. 2019; Grützner et al. 2021). This
166 version of *Cas9* could improve genome editing by enhancing the stability, translation, and expression of
167 *Cas9* (Castel et al. 2019; Grützner et al. 2021). Another potential factor is the nature of the promoters
168 driving gRNAs, which play an important role in regulating expression of the gRNAs (Zhan et al. 2021;
169 Massel et al. 2022). Another might involve incubating tissues at higher temperatures, which might lead to

170 improved editing efficiency (LeBlanc et al. 2018; Milner et al. 2020). Finally, Che et al. (Che et al. 2022)
171 reported that the *Wus2*-integrated transformation strategy resulted in improved CRISPR/*Cas9* gene
172 dropout frequency, possibly due to enhanced cell division and/or chromatin accessibility.
173
174 In our work, different treatments were incorporated that could lead to improved genome editing and
175 knockout efficiencies, as described above. These include using the *Wus2*-integrated transformation
176 strategy, a maize codon-optimized and intronized *Cas9*, monocistronic and/or polycistronic tRNA-gRNA
177 expression cassettes, and/or the *SbU6* 2.3 and *SbU6* 3.1 promoters driving gRNAs. Effects of two
178 temperature conditions, 25°C and 28°C, during culturing of tissues were also tested.
179
180 To assess the impact of the totality of these various factors, *SbPDS* was amplified from transgenic plants
181 and characterized using Sanger sequencing to study the nature of the genome edits. Sequencing results
182 were further analyzed using the Synthego ICE tool. The editing efficiency of the edited plants, referring to
183 the knockout score, ranged from 0% to 100% (**Figure 3C**). Observed albino phenotypes **(Figure 3B)** were
184 used to visually identify plants with *SbPDS* gene knockouts and to calculate knockout efficiency. Based on
185 these analyses, it appears that, by combining the effects of all of these factors, editing and knockout
186 efficiencies greatly improved over those seen in our previous publication, which was 22.6% and 16.7%
187 ((Aregawi et al. 2022)). When considering one plant per IE, the monocistronic strategy yielded a very high
188 editing and knockout efficiency of approximately 100% (**Table 1)**. Treating tissues at 28°C, compared to
189 25°C, showed no difference in editing and knockout scores. Although lower than the monocistronic
190 strategy, the polycistronic strategy still resulted in relatively high editing efficiencies of 76.6% and 88.5%
191 at 28°C and 25°C conditions, respectively (**Table 1)**. Most edited plants had a small, 1- or 2-bp deletion
192 upstream of the PAM region (**Figure 3D**). Only a small number (16.7 %) showed larger (~5-bp) deletions
193 or insertions.
194

195 Comparison of plant phenotype with knockout score in *SbPDS* edited
196 plantlets

197 In our study, the *SbPDS* gene was selected as the target for genome editing, with the albino
198 phenotype serving as a visual phenotype for successful gene knockouts. T_0 plants were
199 phenotyped based on the percentage of the albino sectors observed. Fully albino plantlets were

200 scored as 100%, while 0% represented fully green plants. This approach enabled assessment of
201 phenotype, which is not feasible for genes for which knockouts do not produce observable
202 phenotypic changes. Mutations at the target sites were analyzed using Synthego ICE analysis,
203 which uses Sanger sequencing data from amplicons encompassing the potential edited sites. This
204 analysis enabled precise identification and quantification of the types and frequencies of
205 mutations induced by genome editing. For the majority of plants, phenotypic and genotypic
206 scores were closely aligned, with few discrepancies (**Table S2**). The two metrics showed a strong
207 correlation, with a Pearson's correlation coefficient of 0.81. This strong correlation underscores
208 the utility of Synthego ICE as a reliable tool for estimating the nature of genotypic changes,
209 especially in cases where gene knockouts do not manifest visually detectable phenotypes in T_0
210 generation.
211

212 Editing efficiency using PAM-less intronized *Cas9* variant, ZmSpRYi

213 To enhance genome editing capabilities and to identify options with fewer PAM sequence constraints, a
214 range of nucleases were considered, including *Cas9* variants and *Cas9* orthologs (Ge et al. 2019; B. Ren et
215 al. 2019; Zhong et al. 2019; Q. Ren et al. 2021; Xu et al. 2021). Previous studies demonstrated that
216 CRISPR/*Cas9*-mediated editing of promoters can generate diverse cis-regulatory alleles, providing
217 valuable quantitative variation for crop breeding (Rodríguez-Leal et al. 2017; Zhou et al. 2023; Patel-
218 Tupper et al. 2024). However, the standard CRISPR/*Cas9* system relies on canonical gRNAs with NGG as
219 the PAM sequence, posing a significant limitation since promoter regions are typically AT-rich. This
220 restricts the feasibility of targeted editing within cis-regulatory modules.
221
222 To address this restriction, PAM-flexible *Cas9* variants, such as *SpRY* (Walton et al. 2020), were used to
223 enable targeted promoter editing and to expand genome engineering in AT-rich genomic regions. Building
224 on an intronized *ZmCas9*, targeted mutations were introduced in eleven nucleotides to create a maize
225 codon-optimized *SpRY* variant, *ZmSpRYi*, with an intron for enhanced transcription and translation (**Figure**
226 **4A**).
227
228 Previous studies suggested that *SpRY* activity may be less efficient due to its lack of an NGG PAM
229 requirement (Hibshman et al. 2024). To evaluate the in vivo editing efficiency of ZmSpRYi, compared with

230 that of ZmCas9i, *ZmCas9i* was substituted with *ZmSpRYi* in constructs to enable a direct comparison using
231 the same gRNAs. Two constructs were designed, featuring polycistronic and monocistronic transcriptional
232 units of gRNAs, and these were transformed into sorghum RTx430. Regenerants from using the
233 monocistronic editing construct (pGL227) exhibited an albino phenotype (**Figure 4B**) as early as four weeks
234 post-Agrobacterium infection, whereas no albino phenotype was observed at that same time with the
235 polycistronic editing construct (pGL226) (**Figure S2**). To assess editing efficiency of ZmSpRYi, all
236 independent transformants were genotyped by PCR amplification, followed by Sanger sequencing.
237 Analysis of the sequencing data using Synthego ICE revealed that, when using the polycistronic
238 transcription system, 17 out of 60 (28.3%) independent transformants were edited, whereas 77 out of 89
239 (86.5%) transformants were edited using the monocistronic system (**Table 2, Figure 4C**). Further analysis
240 showed that the monocistronic system yielded a higher knockout score (**Figure 4E**), suggesting that editing
241 events occur earlier when individual promoters are used to drive gRNA expression. Previous studies
242 demonstrated that *SpRY* exhibits self-editing activity, targeting its own expression cassettes within
243 integrated T-DNA fragments (**Figure 4A**) (Q. Ren et al. 2021; Xu et al. 2021). Here, we analyzed gRNA
244 expression cassettes within T-DNA and self-editing was observed in 1 out of 4 cases for polycistronic
245 transformations and 3 out of 8 cases for monocistronic transformations (**Figure 4D**). These results
246 underscore the enhanced efficiency in sorghum of the monocistronic system for genome editing using
247 *ZmSpRYi*.

248 Discussion

249 Development of efficient, targeted, and versatile genome-editing tools is needed to advance genetic
250 engineering and editing in bioenergy crops like sorghum. As a C4 plant, sorghum is naturally efficient in
251 photosynthesis and additionally it is highly resilient to environmental stresses, such as drought, flooding,
252 and salinity (Varoquaux et al. 2019). However, the molecular mechanisms underlying such key agronomic
253 traits and the validation of appropriate genetic resources remain significant challenges. To address these
254 issues and enable functional gene analysis while introducing desirable genetic variations in sorghum, we
255 developed a shuttle-binary vector toolbox to address the current limitations of genome editing. This
256 system simplifies genetic engineering by incorporating into the construct the morphogenic gene *Wus2*,
257 which accelerates optimized delivery of editing machinery. Additionally, several optimizations were
258 introduced to improve the efficiency of CRISPR/Cas9-based genome editing in sorghum. These included a
259 codon-optimized Cas9 containing an intron, high-efficiency endogenous U6 promoters, and monocistronic

260 gRNA expression cassettes. These modifications addressed previous limitations and significantly expanded the
261 potential applications of this genome editing technology in sorghum.

262 Using Wuschel integration simplifies the binary vector and improves 263 transformation frequency

264 Previous studies demonstrated that the morphogenic regulators, BBM and WUS2, significantly enhance
265 transformation frequency in monocot plants, including sorghum (Lowe et al. 2016; Aregawi et al. 2022).
266 However, continued integration of these regulators often results in developmental aberrations during the
267 vegetative stage. To address this issue, the CRE/LoxP recombination system was employed to excise these
268 regulators, following somatic embryo initiation (Lowe et al. 2016). While effective, this approach increases
269 binary vector size, complicating molecular cloning and construct development. Efforts to overcome this
270 challenge include development of systems that combine transient and stable *Wus2* expression (Hoerster
271 et al. 2020), reducing construct size. In our approach, we redesigned the binary vector into a more
272 versatile delivery platform by incorporating the LR recombination site, making it compatible with the
273 Gateway system used frequently among plant biotechnologists for construct development. When paired
274 with a *Wus2* expression cassette, we used this system to achieve transformation frequencies of 24 to 42%,
275 comparable to those attained using BBM/WUS2-assisted transformation (Aregawi et al. 2022).
276
277 Despite this success, limitations persist with the integration-based delivery of Wus2. Approximately 10%
278 of the T_0 transformants exhibited developmental deficiencies, such as curly leaves during the vegetative
279 stage, potentially caused by ectopic expression of Wus2. To address this issue, pGL216 was considered as
280 a platform for testing alternative developmental regulators, including Wuschel orthologs from other
281 species or members of the Wuschel homeobox gene family (**Figure 1C**). These alternative candidates may
282 enhance somatic embryo initiation while minimizing developmental disruptions, offering a more refined
283 approach to transformation and regeneration.
284

285 # Optimizing *Cas9* and guide RNA expression cassettes increases editing
286 efficiency

287 In our previous work, we successfully achieved *PDS* knockouts in sorghum using CRISPR/*Cas9*, with an
288 editing efficiency of 16.7% (Aregawi et al. 2022). However, enhancing genome-editing efficiency further
289 requires overcoming certain challenges, particularly ensuring robust expression of the editing machinery,
290 including *Cas9* protein and gRNAs (Liu, Li, and Godwin 2019). To address these challenges, we used a
291 constitutive promoter to drive an intronized maize codon-optimized Cas9 (Che et al., 2022). Intronization
292 has been shown to enhance protein abundance at both transcriptional and translational levels in
293 Arabidopsis (Grützner et al. 2021). For gRNA expression optimization, we utilized the sorghum
294 endogenous snoRNA U6 promoters, which lead to high gRNA expression levels (Massel et al. 2022).
295
296 Previous studies suggest that transcriptional differences between polycistronic and monocistronic gRNA
297 transcription units can affect editing efficiency (Liang et al. 2021). However, it remains unclear in sorghum
298 whether polycistronic transcription units compromise editing efficiency. To investigate this, we conducted
299 a side-by-side comparison of polycistronic versus monocistronic gRNA transcription units. Analysis of
300 results demonstrate that the monocistronic gRNA transcription unit achieved significantly higher editing
301 efficiency, up to 91 to 100%, compared to 58.5 to 92% for the polycistronic unit. This indicates that
302 temporal processing of exogenous tRNA may be compromised during the early embryonic development
303 of cultured tissue. We also observed that the albino phenotypes resulting from PDS knockouts were
304 delayed when using the polycistronic gRNA transcription unit. This delay further supports the notion that
305 transcriptional processing inefficiencies might underlie the reduced editing efficiency associated with
306 polycistronic gRNA systems in sorghum. To further investigate this, we assembled a collection of monocot
307 snoRNA promoters, including U6 promoters from sorghum, wheat, and maize, as well as U3 promoters
308 from wheat and rice (**Figure S1**). These promoters have been experimentally validated in their respective
309 monocot species. Level 0 constructs, using these promoters, offer versatile options for combining multiple
310 gRNAs, enabling simultaneous editing of multiple genomic targets. This approach holds promise for
311 applications, such as promoter editing and other complex genetic modifications.
312
313 To evaluate the impact of temperature on editing efficiency, we conducted an editing experiment under
314 in vitro tissue culture conditions. Incubation temperature following Agrobacterium infection was
315 increased from 25°C to 28°C. Interestingly, no apparent difference in editing efficiency was observed

316 between the two temperatures (**Table 1**). This outcome may be attributed to the high baseline editing
317 efficiency achieved through the modifications made to the Cas9 and gRNA elements. As a result, the
318 elevated temperature did not provide additional improvements in editing, likely because the system was
319 already operating near its optimal efficiency. Also, tissues were healthier, and the number of regenerants
320 appears to be higher at 25 °C. (**Figure S3**). Based on these findings, we suggest 25°C as a more suitable
321 incubation temperature for efficient genome editing in sorghum.

322 Expanding the Scope of Genome Editing and Applications Using ZmSpRYi

323 One potentially impactful application of genome editing in crops is creating cis-regulatory variations to
324 diversify genetic resources for improving desirable traits (Rodríguez-Leal et al. 2017). Cis-regulatory
325 editing in promoters and untranslated regions (UTRs), which are typically AT-rich, is often limited, when
326 using Cas9, because of the strict requirement for NGG PAM sequences. To address this limitation, we
327 considered several potential genome editing candidates to target AT-rich regions, including Cas9 variants
328 (Cas9-NG, xCas9, and SpRY) and other Cas orthologs (Cas12a and Cas12b), which exhibit reduced
329 dependency on CG content at the PAM site (Zetsche et al. 2015; Nishimasu et al. 2018; Hu et al. 2018;
330 Strecker et al. 2019; Walton et al. 2020). Among these, SpRY demonstrated the highest flexibility due to
331 its PAM-less feature (Q. Ren et al. 2021; Xu et al. 2021).
332
333 Using the same gRNAs targeting the PDS gene, as in our previous *Cas9* experiments (Aregawi et al. 2022),
334 Zm*SpRY*i achieved a genotypic editing efficiency of 86.5%. However, previous studies suggested that use
335 of *SpRY* results in compromised double-strand break activity, particularly with non-NGG PAM sequences
336 (Q. Ren et al. 2021). To further investigate ZmSpRYi activity with non-NGG PAM sequences, we are
337 currently examining its performance in combination with WUS2. Previous research indicated that
338 integration of *Wus2* can enhance CRISPR/*Cas9*-mediated gene dropout frequency (Che et al. 2022).
339 However, it remains unclear as to whether *Wus2* integration can similarly enhance SpRY activity. To
340 address this question, we designed six gRNAs targeting the promoter, 5' UTR, and exons of the PDS gene
341 and are currently transforming sorghum with the appropriate editing constructs.
342
343 Another concern for SpRY is the potential for off-target effects, including self-editing. Self-editing refers
344 to mutagenesis occurring within the gRNA expression cassette (Q. Ren et al. 2021; Xu et al. 2021), which
345 could lead to unintended edits. To assess this risk in edits with high knockout scores we amplified and

346 sequenced potential off-target sites, including within the T-DNA region. We examined potential self-
347 editing regions and found that 25.0% to 37.5% of selected edits exhibited self-editing within the T-DNA
348 fragments (unpublished data). Notably, the target regions were also successfully edited in these cases,
349 suggesting that self-editing occurred either concurrently or sequentially with the targeted editing process.
350 The present study highlights the promise of *SpRY* for expanding the genome editing toolbox in AT-rich
351 regions while addressing challenges, such as compromised activity and off-target risks.
352
353 In this study, we developed a high-efficiency editing platform incorporating *wus2* integration with a robust
354 Cas9-based genome editing toolkit, featuring intronized ZmCas9 and ZmSpRY. This transformation
355 platform is a versatile tool for delivering genome editing machinery that can include base editors and
356 prime editors. By integrating *wus2* with the SpRY Cas9 variant, we expanded the editing scope to enable
357 other desirable applications, such as enabling promoter editing. These advancements provide a
358 streamlined approach to generating diverse genetic variation, facilitating crop improvement efforts that
359 address food security challenges and contribute to carbon capture initiatives that are addressing climate
360 change.
361

362 Materials and Methods

363 Plant material and growth conditions

364 Seeds of *Sorghum bicolor* genotype RTx430 were sourced from the Germplasm Resources Information
365 Network (GRIN, USDA-ARS, PI 655998). Plants were cultivated in three-gallon pots containing SuperSoil in
366 the Oxford Research Unit South Greenhouse, under controlled conditions of 30°C/24°C (day/night) with a
367 16-hour light/8-hour dark photoperiod. Immature embryos (IEs) were harvested 12–14 days post-
368 anthesis.

369 Construct creation

370 To create pGL206, the hygromycin phosphotransferase gene (*hph*), driven by the *Panicum virgatum*
371 *Ubiquitin2* promoter (PvUbi2p), was amplified from pANIC10A (Mann et al. 2012) using the primer SorEd1
372 and 2 (**Table S1**). All primers used for construct building are described in **Table S1.** The terminator of

373 sorghum PEPC was amplified from pPHP85425 (Aregawi et al. 2022) using the primers SorEd3 and 4.
374 These two parts were assembled by overlapping PCR. The vector backbone of pPHP85425 was amplified
375 using the primers SorEd5 and 6. In addition, the Buffer3 and attR4-attR3 fragments were amplified from
376 pPHP85425 using the primers SorEd7 and 8. These three fragments were assembled using Gibson
377 assembly (NEBuilder® HiFi DNA Assembly Master Mix). To construct pGL216, the *ZsG* expression cassette
378 was amplified from pGL190 using the primer SorEd9 and 10. The amplified cassette was then inserted into
379 pGL206 through *Sfi*I digestion and subsequent ligation. To create pGL222, the partial backbone of
380 pPHP96564 (Che et al. 2022) and the *Wus2* expression cassette were amplified from pPHP96564 using the
381 primers SorEd11 and 12. The attR4-attR3 region was amplified from pPHP85425 (Aregawi et al. 2022)
382 using the primers SorEd13 and 14. The *hygromycin B phosphotransferase* gene was amplified from pGL206
383 using the primers SorEd15 and 16. The rest of the backbone of pPHP96564 was amplified with the primers
384 SorEd17 and 18. These fragments were reassembled into the final vector using Gibson assembly.
385 Additionally, the *ZsG* gene, driven by the *Sorghum bicolor ubiquitin1* promoter, was amplified from
386 pGL190 (Aregawi et al. 2022) with the primers SorEd19 and 20. The ZsG expression cassette was digested
387 by *Nhe*I and *Pme*I and ligated into the construct to finalize the construct, pGL222; it was validated using
388 Nanopore sequencing.
389
390 To optimize shuttle constructs, the sorghum U6.2.3 (SbU6.2.3) promoter (Massel et al. 2022) from
391 sorghum genotype RTx430 was amplified using the primers SorEd-21 and 22. pGL198 (Aregawi et al. 2022)
392 was linearized by primers, SorEd-23 and 24. The OsU3 promoter was replaced by SbU6.2.3 using Gibson
393 Assembly. Additionally, ZmCas9 was replaced by ZmCas9i using primers SorEd25 and 26 for vector
394 linearization and primers SorEd27 and 28 for ZmCas9i amplification from pPHP86564, resulting in the
395 shuttle vector, pGL220. Based on the polycistronic shuttle vector construction, the monocistronic shuttle
396 vector was created by inserting two gRNA expression cassettes by Gibson assembly with primers SorEd29-
397 36 to create the monocistronic expression cassettes. Cas9 and gRNA polycistronic and monocistronic
398 cassettes were transferred to pGL222 to create binary constructs pGL220 and 221 by LR recombination.
399 To create pGL224, we used the same strategy to replace the OsU3 promoter and ZmCas9 with the
400 SbU6.2.3 promoter and ZmCas9i as described above. To streamline construct creation, level 0 constructs
401 were developed. These constructs were created by fusing the gRNA scaffold with various snoRNA
402 promoters (including sorghum U6_2.3 [SbU6_2.3], sorghum U6_3.1 [SbU6_3.1], rice U3 [OsU3], maize U6
403 [ZmU6], wheat U3 [TaU3], and wheat U6 [TaU6]) using overlapping PCR with primers SorEd49 through 62.
404 Fused DNA fragments were cloned into a pJET1.2 vector using CloneJET PCR cloning kit (ThermoFisher

405 Scientific) and validated by Sanger sequencing. These level 0 constructs served as templates for creating
406 both polycistronic and monocistronic gRNA editing constructs (**Figure S2**).
407
408 To create the ZmSpRYi construct, pGL224 was used as the template, and a total of 14 nucleotide mutations
409 were introduced. The first set of mutations on the first exon of ZmCas9i targeted the removal of a BsaI
410 recognition site and the substitution of the alanine 61 with an arginine. These mutations were
411 incorporated using primers SorEd37 and SorEd38, enabling the amplification of two overlapping
412 fragments with primers SorEd39 and SorEd40. The overlapping fragments were assembled through
413 overlapping PCR. The modified sequence replaced the original sequence via BamHI and BspEI digestion,
414 followed by ligation. The remaining ten mutations were introduced using a synthetic oligonucleotide
415 chemically synthesized by Genewiz (http://genewiz.com). These mutations were inserted into the 3' end
416 of ZmCas9i through Gibson assembly. Primers SorEd41 and SorEd42 were used to amplify the insert, while
417 primers SorEd43 and SorEd44 were employed for vector linearization. Additionally, two unwanted BsaI
418 restriction sites were eliminated via primer-directed mutagenesis using primers SorEd45 through
419 SorEd48, resulting in the construct, pGL225 (**Figure S1**). Finally, the ZmCas9i gene in pGL220 and pGL221
420 was replaced with the ZmSpRYi gene to create pGL226 and pGL227, designed for Agrobacterium-mediated
421 transformation
422

423 Agrobacterium-mediated transformation

424 The binary constructs were introduced into an auxotrophic strain of *Agrobacterium tumefaciens* LBA4404
425 Thy- (Anand et al. 2017) by electroporation. Transformed Agrobacterium strains were plated on yeast
426 extract peptone (YEP) medium supplemented with 100 mg/L thymidine, 50 mg/L gentamicin, and 50 mg/L
427 spectinomycin. Details on the storage and preparation of the Agrobacterium strains follow a previously
428 published protocol (Masters et al. 2020). In summary, Agrobacterium stocks were streaked onto YEP
429 plates containing appropriate antibiotics to generate master plates. After a 2-day incubation at 28°C, 5–6
430 colonies from the master plates were selected to establish working cultures on YEP plates. Following
431 overnight incubation and just prior to inoculation of sorghum immature embryos, Agrobacterium
432 suspensions were prepared in PHI-I medium (Wu et al. 2014), with optical density (OD550 nm), adjusted
433 to 0.7; silwet L-77 (0.005% v/v) and acetosyringone (0.2 mM) were added to finalize the Agrobacterium

434 inoculation medium. Transformation frequency refers to the percentage of IEs used in the transformation
435 that successfully produce transformants.

436 Visualization of T-DNA integration

437 The ZsGreen reporter gene was used as a visible marker to track T-DNA integration and segregation. To
438 monitor T-DNA integration following Agrobacterium-mediated inoculation, transformed IEs were
439 examined weekly using a Lumar v12 epifluorescence stereo microscope and a QImaging Retiga SRV
440 camera (Zeiss, UC Berkeley Biological Imaging Facility). The response of IEs to WUS expression was
441 assessed by analyzing the number and size of fluorescent tissues. Prior to transferring shoots to rooting
442 medium, regenerants exhibiting fluorescence were selected for further genotyping and phenotyping.

443 Phenotypic characterization of T_0 transgenic plants

444 T_0 plantlets were phenotyped while growing in rooting medium. Each plantlet was scored for the
445 percentage of albino phenotype, with 100% indicating plants that were completely albino and 0%
446 indicating plants that were completely green. The phenotype score was compared with the knockout
447 percentage obtained using the Synthego Inference of CRISPR Edits (ICE) tool (Conant et al. 2022) to
448 determine correlation between the two observations.

449 Genotyping of editing events

450 To test putative T_0 transgenic lines for successful editing of target genes, genomic DNA from young
451 sorghum leaves was isolated using a urea buffer as described (Aregawi et al. 2022). Target regions of
452 potential edits were amplified using the primers SorEd63 and 64 and purified with the GeneJet PCR
453 Purification Kit (Thermo Scientific). Purified PCR products were sequenced with Sanger sequencing at the
454 UC Berkeley DNA Sequencing Facility. Sequencing data were analyzed using the Synthego ICE analysis tool
455 (Conant et al. 2022), and knockout scores, referring to proportion of indels that indicate a frameshift or
456 are more than 21 bp in length, were used to assess editing efficiency and the likelihood of transmission to
457 the next generation. The editing efficiency represents the percentage of plant cells within harvested
458 somatic samples that successfully undergo knockout events, as determined by the knockout score.

Acknowledgments

This project was supported by the Chan-Zuckerberg Initiative and the DOE EERC project through the Lawrence Livermore National Laboratory. PGL acknowledges support from the US Cooperative Extension Service through the Division of Agriculture and Natural Resources of the University of California. JS acknowledges support from USDA-ARS Crop Improvement and Genetics Unit Albany, CA and ORISE Research Participation Program. We thank Dr. William Gordon-Kamm at Corteva Agriscience for helpful conversations and for the constructs, pPHP96564 and pPHP85425. We thank Dr. Roger Thilmony at USDA-ARS Crop Improvement and Genetics Unit Albany for informative discussions. We thank talented undergraduate students, Malia Ariyoshi, Emma To, Eda Joy Ustuner and Mantra Rajkumar, for their help in this work. We are grateful for the help of the staff of the UC Berkeley Biological Imaging Facility and the UC Berkeley Oxford Tract Greenhouse Facility.

References

Altpeter, Fredy, Nathan M. Springer, Laura E. Bartley, Ann E. Blechl, Thomas P. Brutnell, Vitaly Citovsky, Liza J. Conrad, et al. 2016. "Advancing Crop Transformation in the Era of Genome Editing." *The Plant Cell* 28 (7): 1510–20.

Aregawi, Kiflom, Jianqiang Shen, Grady Pierroz, Manoj K. Sharma, Jeffery Dahlberg, Judith Owiti, and Peggy G. Lemaux. 2022. "Morphogene-Assisted Transformation of Sorghum Bicolor Allows More Efficient Genome Editing." *Plant Biotechnology Journal* 20 (4): 748–60.

Anand, A., Bass, S.H., Cho, H.-J., Klein, T.M., Lassner, M., McBridge, K.E. 2017. Methods and Compositions of Improved Plant Transformation. WIPO 2017/078836 Al. World Patent, filed August 26, 2016, and issued November 5, 2017.

Blomme, Jonas, Ward Develtere, Ayse Köse, Júlia Arraiza Ribera, Christophe Brugmans, Jessica Jaraba-Wallace, Ward Decaestecker, et al. 2022. "The Heat Is on: A Simple Method to Increase Genome Editing Efficiency in Plants." *BMC Plant Biology* 22 (1): 142.

Castel, Baptiste, Laurence Tomlinson, Federica Locci, Ying Yang, and Jonathan D. G. Jones. 2019. "Optimization of T-DNA Architecture for Cas9-Mediated Mutagenesis in Arabidopsis." *PloS One* 14 (1): e0204778.

Che, Ping, Emily Wu, Marissa K. Simon, Ajith Anand, Keith Lowe, Huirong Gao, Amy L. Sigmund, et al. 2022. "Wuschel2 Enables Highly Efficient CRISPR/Cas-Targeted Genome Editing during Rapid de Novo Shoot Regeneration in Sorghum." *Communications Biology* 5 (1): 344.

Conant, David, Tim Hsiau, Nicholas Rossi, Jennifer Oki, Travis Maures, Kelsey Waite, Joyce Yang, et al. 2022. "Inference of CRISPR Edits from Sanger Trace Data." *The CRISPR Journal* 5 (1): 123–30.

Dahlberg, J. A., J. J. Burke, and D. T. Rosenow. 2004. "Development of a Sorghum Core Collection: Refinement and Evaluation of a Subset from Sudan." *Economic Botany* 58 (4): 556–67.

494 Elzen, P. J. van den, J. Townsend, K. Y. Lee, and J. R. Bedbrook. 1985. "A Chimaeric Hygromycin
495 Resistance Gene as a Selectable Marker in Plant Cells." *Plant Molecular Biology* 5 (5): 299–302.
496 Ge, Zengxiang, Leiqi Zheng, Yuling Zhao, Jiahao Jiang, Emily J. Zhang, Tianxu Liu, Hongya Gu, and Li-Jia
497 Qu. 2019. "Engineered XCas9 and SpCas9-NG Variants Broaden PAM Recognition Sites to
498 Generate Mutations in Arabidopsis Plants." *Plant Biotechnology Journal* 17 (10): 1865–67.
499 Grützner, Ramona, Patrick Martin, Claudia Horn, Samuel Mortensen, Erin J. Cram, Carolyn W. T. Lee-
500 Parsons, Johannes Stuttmann, and Sylvestre Marillonnet. 2021. "High-Efficiency Genome Editing
501 in Plants Mediated by a Cas9 Gene Containing Multiple Introns." *Plant Communications* 2 (2):
502 100135.
503 Hibshman, Grace N., Jack P. K. Bravo, Matthew M. Hooper, Tyler L. Dangerfield, Hongshan Zhang, Ilya J.
504 Finkelstein, Kenneth A. Johnson, and David W. Taylor. 2024. "Unraveling the Mechanisms of
505 PAMless DNA Interrogation by SpRY-Cas9." *Nature Communications* 15 (1): 3663.
506 Hoerster, George, Ning Wang, Larisa Ryan, Emily Wu, Ajith Anand, Kevin McBride, Keith Lowe, Todd
507 Jones, and Bill Gordon-Kamm. 2020. "Use of Non-Integrating Zm-Wus2 Vectors to Enhance
508 Maize Transformation." *In Vitro Cellular & Developmental Biology. Plant: Journal of the Tissue*
509 *Culture Association* 56 (3): 265–79.
510 Hu, Johnny H., Shannon M. Miller, Maarten H. Geurts, Weixin Tang, Liwei Chen, Ning Sun, Christina M.
511 Zeina, et al. 2018. "Evolved Cas9 Variants with Broad PAM Compatibility and High DNA
512 Specificity." *Nature* 556 (7699): 57–63.
513 Jinek, Martin, Krzysztof Chylinski, Ines Fonfara, Michael Hauer, Jennifer A. Doudna, and Emmanuelle
514 Charpentier. 2012. "A Programmable Dual-RNA-Guided DNA Endonuclease in Adaptive Bacterial
515 Immunity." *Science (New York, N.Y.)* 337 (6096): 816–21.
516 Jores, Tobias, Jackson Tonnies, Travis Wrightsman, Edward S. Buckler, Josh T. Cuperus, Stanley Fields,
517 and Christine Queitsch. 2021. "Synthetic Promoter Designs Enabled by a Comprehensive
518 Analysis of Plant Core Promoters." *Nature Plants* 7 (6): 842–55.
519 LeBlanc, Chantal, Fei Zhang, Josefina Mendez, Yamile Lozano, Krishna Chatpar, Vivian F. Irish, and
520 Yannick Jacob. 2018. "Increased Efficiency of Targeted Mutagenesis by CRISPR/Cas9 in Plants
521 Using Heat Stress." *The Plant Journal: For Cell and Molecular Biology* 93 (2): 377–86.
522 Lee, Jeong Sun, Su-Ji Bae, Jin-Soo Kim, Changsoo Kim, and Beum-Chang Kang. 2023. "A Streamlined
523 Guide RNA Screening System for Genome Editing in Sorghum Bicolor." *Plant Methods* 19 (1): 90.
524 Liang, Zhen, Yuqing Wu, Lingling Ma, Yingjie Guo, and Yidong Ran. 2021. "Efficient Genome Editing in
525 Setaria Italica Using CRISPR/Cas9 and Base Editors." *Frontiers in Plant Science* 12: 815946.
526 Liu, Guoquan, Jieqing Li, and Ian D. Godwin. 2019. "Genome Editing by CRISPR/Cas9 in Sorghum through
527 Biolistic Bombardment." *Methods in Molecular Biology (Clifton, N.J.)* 1931: 169–83.
528 Lowe, Keith, Mauricio La Rota, George Hoerster, Craig Hastings, Ning Wang, Mark Chamberlin, Emily
529 Wu, Todd Jones, and William Gordon-Kamm. 2018. "Rapid Genotype 'Independent' Zea Mays L.
530 (Maize) Transformation via Direct Somatic Embryogenesis." *In Vitro Cellular & Developmental*
531 *Biology. Plant: Journal of the Tissue Culture Association* 54 (3): 240–52.
532 Lowe, Keith, Emily Wu, Ning Wang, George Hoerster, Craig Hastings, Myeong-Je Cho, Chris Scelonge, et
533 al. 2016. "Morphogenic Regulators Baby Boom and Wuschel Improve Monocot Transformation."
534 *The Plant Cell* 28 (9): 1998–2015.
535 Mann, David G. J., Peter R. Lafayette, Laura L. Abercrombie, Zachary R. King, Mitra Mazarei, Mathew C.
536 Halter, Charleson R. Poovaiah, et al. 2012. "Gateway-Compatible Vectors for High-Throughput
537 Gene Functional Analysis in Switchgrass (Panicum Virgatum L.) and Other Monocot Species."
538 *Plant Biotechnology Journal* 10 (2): 226–36.
539 Massel, Karen, Yasmine Lam, Jessica Hintzsche, Nicholas Lester, Jose R. Botella, and Ian D. Godwin. 2022.
540 "Endogenous U6 Promoters Improve CRISPR/Cas9 Editing Efficiencies in Sorghum Bicolor and
541 Show Potential for Applications in Other Cereals." *Plant Cell Reports* 41 (2): 489–92.

542 Masters, Alicia, Minjeong Kang, Morgan McCaw, Jacob D. Zobrist, William Gordon-Kamm, Todd Jones,
543 and Kan Wang. 2020. "Agrobacterium-Mediated Immature Embryo Transformation of
544 Recalcitrant Maize Inbred Lines Using Morphogenic Genes." *Journal of Visualized Experiments:*
545 *JoVE*, no. 156 (February): e60782.
546 Milner, Matthew J., Melanie Craze, Matthew S. Hope, and Emma J. Wallington. 2020. "Turning up the
547 Temperature on CRISPR: Increased Temperature Can Improve the Editing Efficiency of Wheat
548 Using CRISPR/Cas9." *Frontiers in Plant Science* 11 (November): 583374.
549 Milner, Matthew J., Manisha Sharma, Ruth E. Bates, Michelle Whiting, Melanie S. Craze, Peter Miller,
550 Jack Brooks, Allan Kouidri, and Emma J. Wallington. 2024. "Differential Editing Efficiencies in
551 Cereal Crops: A Comparative Analysis of TRNA and Ribozyme Multiplexed Guide Delivery."
552 *Frontiers in Plant Science* 15 (December): 1426184.
553 Ming, Meiling, Qiurong Ren, Changtian Pan, Yao He, Yingxiao Zhang, Shishi Liu, Zhaohui Zhong, et al.
554 2020. "CRISPR-Cas12b Enables Efficient Plant Genome Engineering." *Nature Plants* 6 (3): 202–8.
555 Nishimasu, Hiroshi, Xi Shi, Soh Ishiguro, Linyi Gao, Seiichi Hirano, Sae Okazaki, Taichi Noda, et al. 2018.
556 "Engineered CRISPR-Cas9 Nuclease with Expanded Targeting Space." *Science (New York, N.Y.)*
557 361 (6408): 1259–62.
558 Patel-Tupper, Dhruv, Armen Kelikian, Anna Leipertz, Nina Maryn, Michelle Tjahjadi, Nicholas G.
559 Karavolias, Myeong-Je Cho, and Krishna K. Niyogi. 2024. "Multiplexed CRISPR-Cas9 Mutagenesis
560 of Rice PSBS1 Noncoding Sequences for Transgene-Free Overexpression." *Science Advances* 10
561 (23): eadm7452.
562 Paterson, Andrew H., John E. Bowers, Rémy Bruggmann, Inna Dubchak, Jane Grimwood, Heidrun
563 Gundlach, Georg Haberer, et al. 2009. "The Sorghum Bicolor Genome and the Diversification of
564 Grasses." *Nature* 457 (7229): 551–56.
565 Ramstein, Guillaume P., Sarah E. Jensen, and Edward S. Buckler. 2019. "Breaking the Curse of
566 Dimensionality to Identify Causal Variants in Breeding 4." *Theoretical and Applied Genetics* 132
567 (3): 559–67.
568 Ren, Bin, Lang Liu, Shaofang Li, Yongjie Kuang, Jingwen Wang, Dawei Zhang, Xueping Zhou, Honghui Lin,
569 and Huanbin Zhou. 2019. "Cas9-NG Greatly Expands the Targeting Scope of the Genome-Editing
570 Toolkit by Recognizing NG and Other Atypical PAMs in Rice." *Molecular Plant* 12 (7): 1015–26.
571 Ren, Qiurong, Simon Sretenovic, Shishi Liu, Xu Tang, Lan Huang, Yao He, Li Liu, et al. 2021. "PAM-Less
572 Plant Genome Editing Using a CRISPR-SpRY Toolbox." *Nature Plants* 7 (1): 25–33.
573 Rodríguez-Leal, Daniel, Zachary H. Lemmon, Jarrett Man, Madelaine E. Bartlett, and Zachary B. Lippman.
574 2017. "Engineering Quantitative Trait Variation for Crop Improvement by Genome Editing." *Cell*
575 171 (2): 470-480.e8.
576 Schindele, Angelina, Annika Dorn, and Holger Puchta. 2020. "CRISPR/Cas Brings Plant Biology and
577 Breeding into the Fast Lane." *Current Opinion in Biotechnology* 61 (February): 7–14.
578 Strecker, Jonathan, Sara Jones, Balwina Koopal, Jonathan Schmid-Burgk, Bernd Zetsche, Linyi Gao, Kira S.
579 Makarova, Eugene V. Koonin, and Feng Zhang. 2019. "Engineering of CRISPR-Cas12b for Human
580 Genome Editing." *Nature Communications* 10 (1): 212.
581 Tang, Xu, Levi G. Lowder, Zhang Tao, Aimee A. Malzahn, Xuelian Zheng, D. Voytas, Zhaohui Zhong, et al.
582 2017. "A CRISPR–Cpf1 System for Efficient Genome Editing and Transcriptional Repression in
583 Plants." *Nature Plants* 3 (February). https://doi.org/10.1038/nplants.2017.18.
584 Varoquaux, Nelle, Benjamin Cole, Cheng Gao, Grady Pierroz, Christopher R. Baker, Dhruv Patel, Mary
585 Madera, et al. 2019. "Transcriptomic Analysis of Field-Droughted Sorghum from Seedling to
586 Maturity Reveals Biotic and Metabolic Responses." *Proceedings of the National Academy of*
587 *Sciences of the United States of America* 116 (52): 27124–32.

Walton, Russell T., Kathleen A. Christie, Madelynn N. Whittaker, and Benjamin P. Kleinstiver. 2020. "Unconstrained Genome Targeting with Near-PAMless Engineered CRISPR-Cas9 Variants." *Science (New York, N.Y.)* 368 (6488): 290–96.

Wu, Emily, Brian Lenderts, Kimberly Glassman, Maya Berezowska-Kaniewska, Heather Christensen, Tracy Asmus, Shifu Zhen, Uyen Chu, Myeong-Je Cho, and Zuo-Yu Zhao. 2014. "Optimized Agrobacterium-Mediated Sorghum Transformation Protocol and Molecular Data of Transgenic Sorghum Plants." *In Vitro Cellular & Developmental Biology. Plant: Journal of the Tissue Culture Association* 50 (1): 9–18.

Xu, Ziyan, Yongjie Kuang, Bin Ren, Daqi Yan, Fang Yan, Carl Spetz, Wenxian Sun, Guirong Wang, Xueping Zhou, and Huanbin Zhou. 2021. "SpRY Greatly Expands the Genome Editing Scope in Rice with Highly Flexible PAM Recognition." *Genome Biology* 22 (1): 6.

Zetsche, Bernd, Jonathan S. Gootenberg, Omar O. Abudayyeh, Ian M. Slaymaker, Kira S. Makarova, Patrick Essletzbichler, Sara E. Volz, et al. 2015. "Cpf1 Is a Single RNA-Guided Endonuclease of a Class 2 CRISPR-Cas System." *Cell* 163 (3): 759–71.

Zhan, Xiangqiang, Yuming Lu, Jian-Kang Zhu, and Jose Ramon Botella. 2021. "Genome Editing for Plant Research and Crop Improvement." *Journal of Integrative Plant Biology* 63 (1): 3–33.

Zhang, Yingxiao, Aimee A. Malzahn, Simon Sretenovic, and Yiping Qi. 2019. "The Emerging and Uncultivated Potential of CRISPR Technology in Plant Science." *Nature Plants* 5 (8): 778–94.

Zhong, Zhaohui, Simon Sretenovic, Qiurong Ren, Lijia Yang, Yu Bao, Caiyan Qi, Mingzhu Yuan, et al. 2019. "Improving Plant Genome Editing with High-Fidelity XCas9 and Non-Canonical PAM-Targeting Cas9-NG." *Molecular Plant* 12 (7): 1027–36.

Zhou, Jianping, Guanqing Liu, Yuxin Zhao, Rui Zhang, Xu Tang, Ling Li, Xinyu Jia, et al. 2023. "An Efficient CRISPR-Cas12a Promoter Editing System for Crop Improvement." *Nature Plants* 9 (4): 588–604.

Zhu, Haocheng, Chao Li, and Caixia Gao. 2020. "Applications of CRISPR-Cas in Agriculture and Plant Biotechnology." *Nature Reviews. Molecular Cell Biology* 21 (11): 661–77.

Author contributions

Jianqiang Shen designed the experiments, developed the constructs, conducted sorghum transformations, and contributed to writing and editing. Kiflom Aregawi contributed to discussions on experimental design, performed sorghum transformations, and contributed to writing and editing. Sultana Anwar conducted sorghum transformations and contributed to editing. Tamara Miller contributed to writing and editing. Peggy G. Lemaux supervised the project, secured funding, and contributed to editing.

Competing interest statement

pGL and pPHP vectors are available for research purpose; using the pPHP vectors for commercial applications requires a paid non-exclusive license from Corteva Agriscience. Manuscript authors have no relationship with Corteva Agriscience.

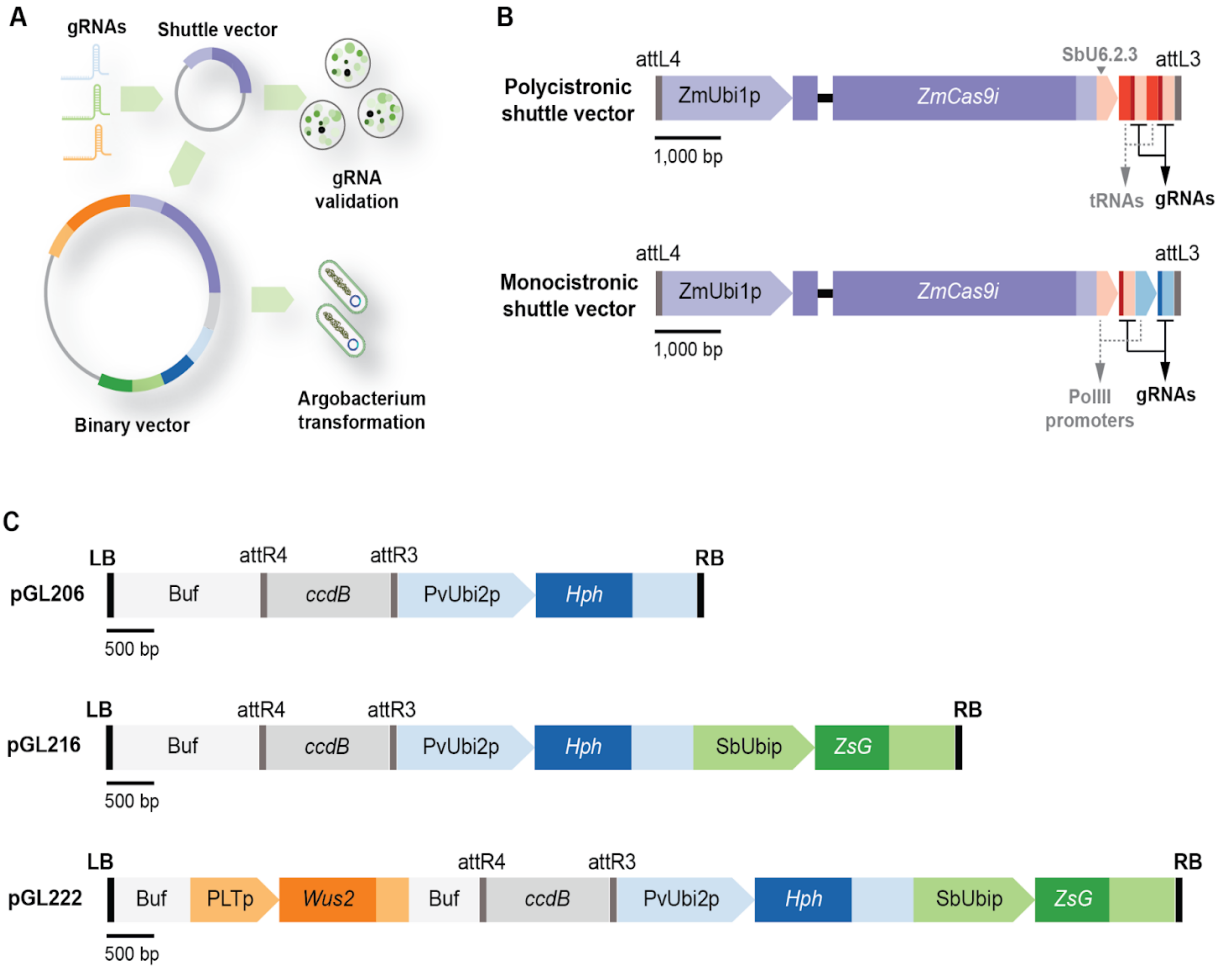

Figure 1. Workflow for construct creation and construct maps.

(A) Diagram illustrating the workflow for construct creation and usage.

(B) Maps of shuttle vectors. Polycistronic shuttle vector contains a polycistronic gRNA transcription unit with tRNA spacers; monocistronic shuttle vector carries monocistronic gRNA transcription units driven by Pol III promoters. Rectangles with arrows indicate promoters. Other rectangles indicate exons (dark-colored) or terminators (light-colored). Black horizontal lines indicate introns. Grey vertical lines indicate Gateway recombination sites.

(C) Maps of binary vectors. pGL206 represents the basic binary vector backbone. pGL216 is designed for testing the function of morphogenic genes in enhancing transformation frequencies. pGL222 is a binary

636 vector backbone used in genome editing applications. Rectangles with arrows indicate promoters. Solid
637 rectangles indicate exons (dark-colored) or terminators (light-colored). Light gray rectangles denote
638 buffer regions; dark gray rectangles represent *ccdB* genes. Black vertical lines indicate T-DNA borders; gray
639 vertical lines indicate Gateway recombination sites.
640

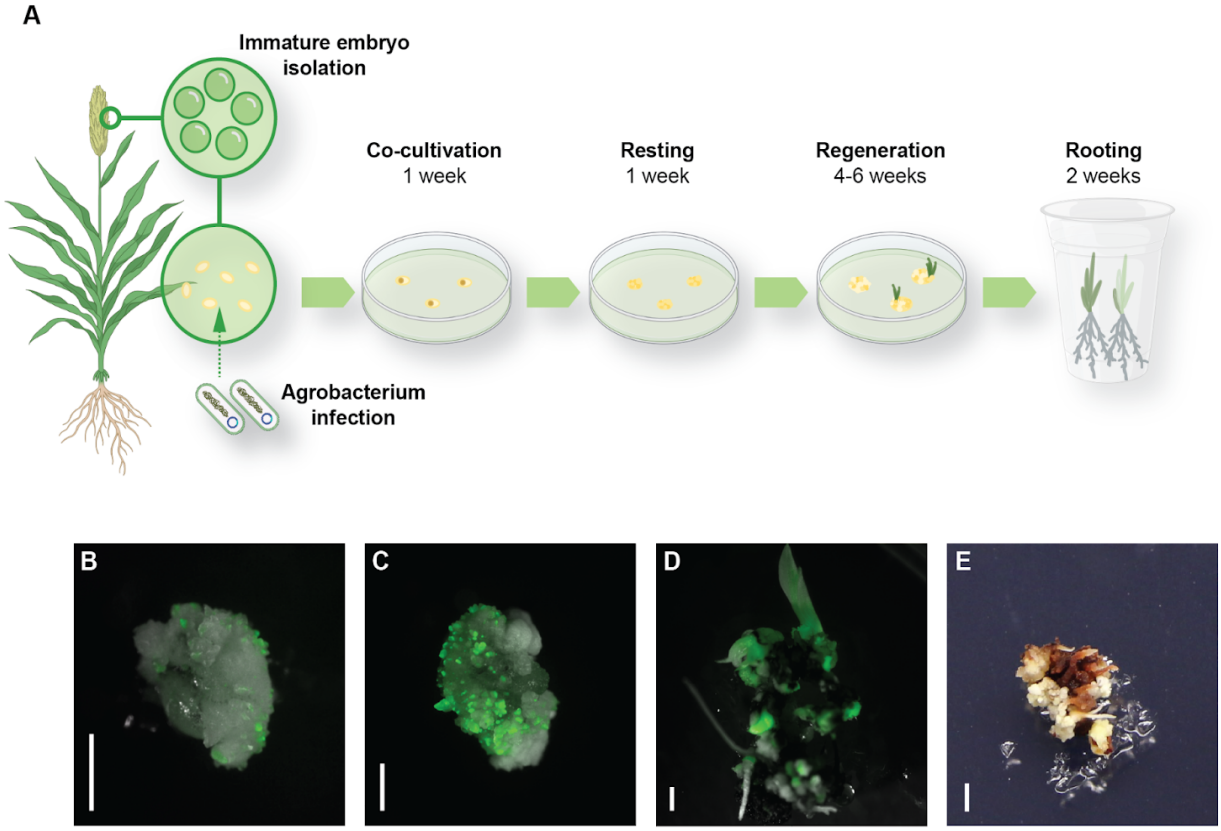

641

642 **Figure 2. Workflow for sorghum immature embryo transformation.**

643 **(A)** Diagram illustrating the transformation workflow, from immature embryo isolation through rooted
644 regenerants.

645 **(B-D)** Sorghum tissues at various stages post-Agrobacterium infection. **(B)** Immature embryos one week
646 after infection; **(C)** two weeks after infection and **(D)** four weeks after infection, visualized with overlays
647 of brightfield and fluorescence images captured with a Zeiss AxioZoom V16 low-magnification
648 epifluorescence microscope. Scale bars indicate 2 mm.

649 **(E)** Sorghum tissue four weeks after Agrobacterium infection, with two weeks of exposure to hygromycin

650 selection. Scale bars indicate 2 mm.

651

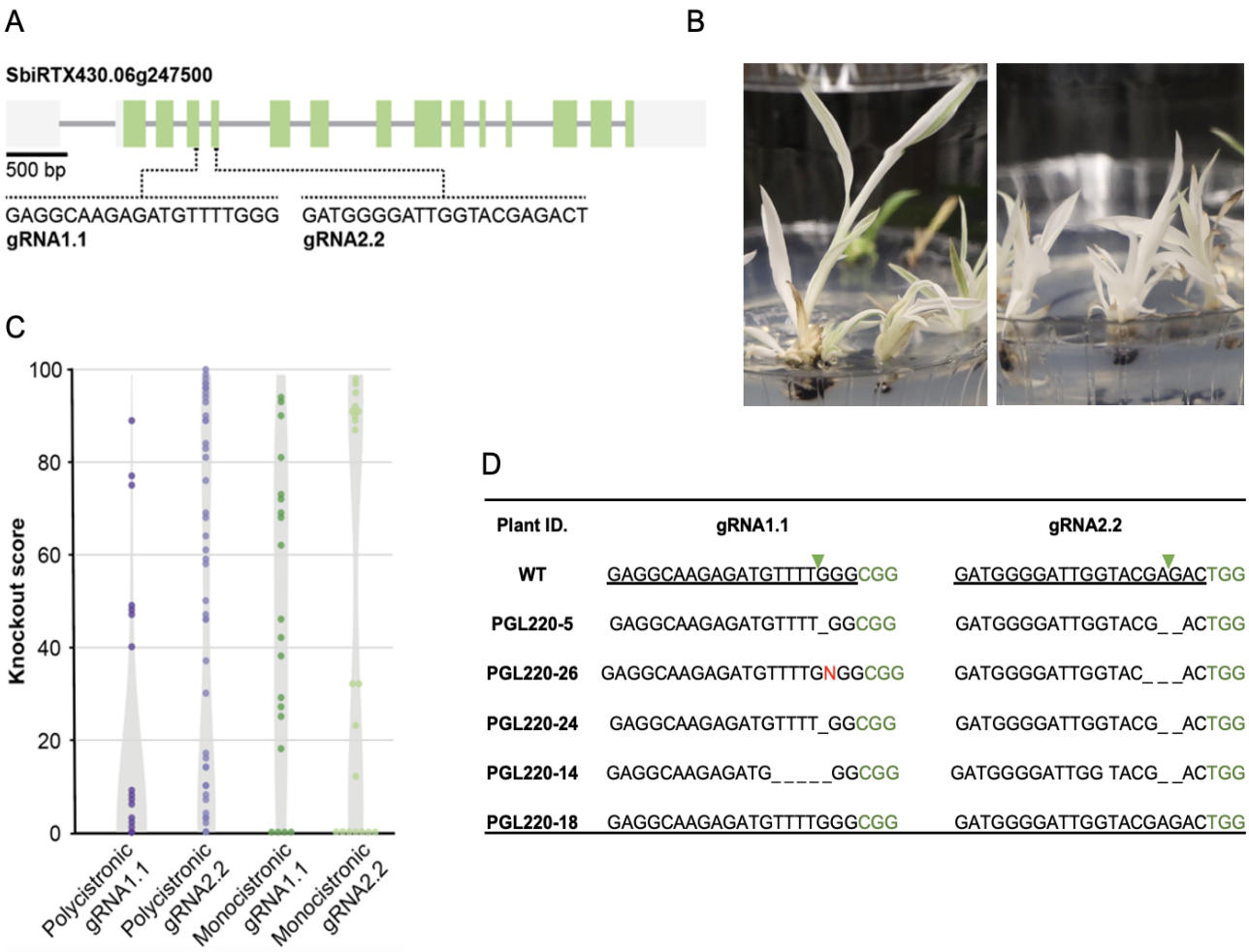

652

653 **Figure 3: Wus2-assisted CRISPR/*Cas9* editing of *SbPDS* gene.**

654 **(A)** Schematic representation of the structure of *SbPDS*, depicting *SbPDS* exons (green boxes) and gRNA target

655 sequences.

656 **(B)** T_0 edited plants showing chimeric (left) and complete (right) albino phenotypes.

657 **(C)** Violin plot showing the distribution of knockout scores obtained from Sanger sequencing and Synthego ICE

658 analysis.

659 **(D)** Sequencing results of targeted regions of *SbPDS* gene in five representative T_0 transgenic plants. gRNAs are

660 underlined, PAM sequences are shown in green, and green triangles indicate cut sites. Dashed lines indicate

661 deletions; insertion is shown in red.

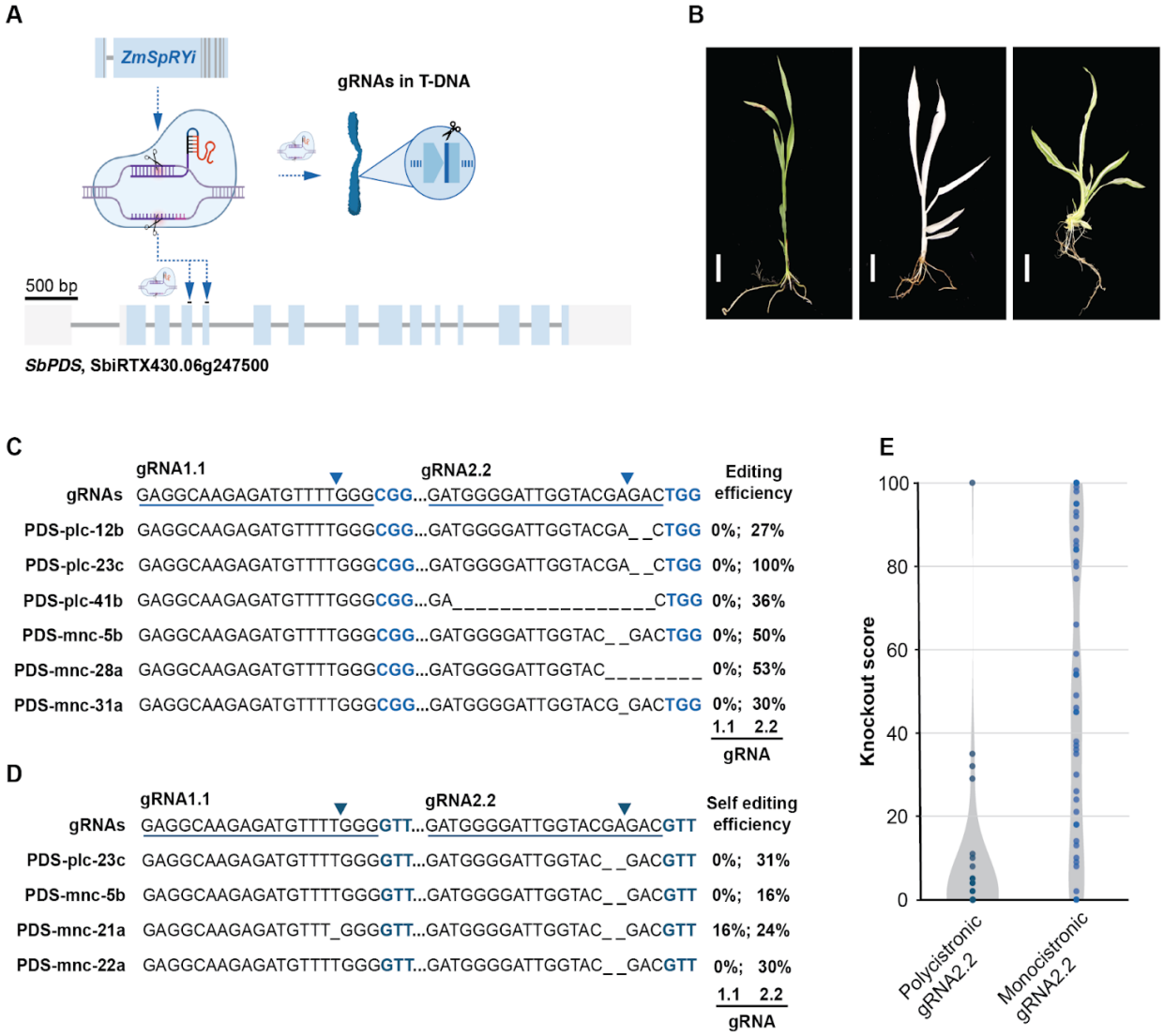

Figure 4. Genome editing in sorghum mediated by CRISPR/SpRY

(A) Diagram illustrating self-editing and genome editing of target sites. Blue rectangles represent exons; gray rectangles denote untranslated regions (UTRs). Gray lines on *ZmSpRYi* indicate mutations. Dark lines above the exons indicate gRNAs. Arrows indicate gene expression or CRISPR/SpRY-mediated editing. **(B)** Phenotypes of PDS gene-edited plants. The left panel shows a non-edited plantlet, the middle panel shows a fully albino plantlet, and the right panel shows a chimeric albino plantlet. Images were taken four weeks after initiation of rooting. Scale bar = 2 cm.

670 **(C)** Genotypes of edited *PDS* gene exons. Underlined sequences indicate gRNA core sequences, triangles
671 represent potential double-strand break sites, and blue-colored nucleotides indicate PAM sequences.
672 Editing efficiency refers to knockout scores in somatic tissues that were genotyped.
673 **(D)** Representative examples of self-editing in gRNA expression cassettes of integrated T-DNA. Underlined
674 sequences indicate gRNA core sequences, triangles represent potential double-strand break sites, and
675 blue-colored nucleotides indicate PAM sequences. Editing efficiency is based on knockout scores from
676 genotyping of somatic tissues.
677 **(E)** Violin plot showing distribution of knockout scores for *PDS* gRNA2.2 edits mediated by CRISPR/*SpRY*,
678 comparing polycistronic and monocistronic gRNA transcription units. For polycistronic units, n = 46; for
679 monocistronic units, n = 49.
680

681 **Table 1.** Transformation, editing and knockout efficiencies of Wus2-assisted transformation based on one
682 plant per IE

gRNA system (Construct)	Temp (°C).	Replication	# IEs used	# Regenerants	# Escapes (%) †	+ for hph ‡	**Transformation frequency (%)** §	# edited plants	**Editing efficiency (%)**¶	# plants with Knockout††	**Knockout efficiency (%)**‡‡
Polycistronic (pGL220)	28	1st	90	40	2(0.05)	38	**42.2**	36	**94.7**	35	**92.0**
		2nd	132	47	6(0.12)	41	**31.0**	24	**58.5**	24	**58.5**
	25	1st	60	26	0(0.00)	26	**43.3**	23	**88.4**	22	**84.6**
Monocistronic (pGL221)	28	1st	93	24	1(0.04)	23	**24.7**	23	**100**	21	**91.3**
		2nd	112	28	1(0.03)	27	**24.1**	27	**100**	27	**100.0**
	25	1st	105	33	1(0.03)	33	**31.4**	33	**100**	33	**100.0**

683 † # Escapes (%) = number and percentage of regenerated plants without transgene (T-DNA) = (#Escapes/# Regenerant) X 100
684 ‡ + = plants PCR-positive for *hph*
685 § Transformation frequency (%) = (# + for *hph* divided by # IEs used) x 100
686 ¶ Editing efficiency (%) = (# edited plants divided by number of plants + for hph) x 100
687 †† # plants with knockout = number of plants with frameshift mutation and albino phenotype
688 ‡‡ Knockout efficiency(%) = (# plants with knockout divided by + for hph) x 100
689

690 **Table 2.** Transformation, editing and knockout efficiencies of Wus2-assisted transformation based on
691 multiple regenerated plants from each IE

gRNA system (Construct)	Temp (ºC).	Replications	# IEs used	# Regenerants	# Escapes (%) †	+ for hph ‡	**Transformation frequency (%)** §	# edited plants	**Editing efficiency (%)** ¶	# plants with Knockout ††	**Knockout efficiency (%)** ‡ ‡
Polycistronic (pGL220)	28	1st	90	82	6 (0.07)	76	**84.4**	68	**89.5**	58	**76.3**
		2nd	132	60	6 (0.1)	54	**40.9**	30	**55.5**	30	**55.5**
	25	1st	60	61	1 (0.02)	60	**100**	51	**85**	48	**80**
Monocistronic (pGL221)	28	1st	93	64	1 (0.02)	63	**67.7**	62	**98.4**	60	**95.2**
		2nd	112	77	3 (0.04)	74	**66.1**	66	**89.2**	63	**85.1**
	25	1st	105	93	6 (0.06)	87	**82.9**	87	**100.0**	84	**96.6**

692 † # Escapes (%) = Number and percentage of regenerated plants without transgene (T-DNA) = (#Escapes/# Regenerant) X
693 100
694 ‡ + indicates plants PCR-positive for *hph*
695 § Transformation frequency (%) = (+ for *hph* divided by # IEs used) x 100
696 ¶ Editing efficiency (%) = (# edited plants divided by number of plants + for hph) x 100
697 †† # plants with knockout = Number of plants with frameshift mutation and albino phenotype
698 ‡‡ Knockout efficiency(%) = (# plants with knockout divided by # + for hph) x 100
699

700 **Table 3.** Transformation, editing and knockout efficiencies of *SpRY* using *Wus2*-assisted transformation
701 strategy

gRNA system (Construct)	Replications	# IEs used	# Regenerants	# Escapes (%) †	+ for hph ‡	**Transformation frequency (%)** §	# edited plants	**Editing efficiency (%)** ¶	# plants with Knockout ††	**Knockout efficiency (%)** ‡ ‡
Polycistronic (pGL226)	1st	107	46	3	43	**40.2**	11	**25.6**	11	**25.6**
	2nd	60	20	3	17	**28.3**	6	**35.3**	6	**35.3**
Monocistronic (pGL227)	1st	119	49	0	49	**41.2**	40	**81.6**	40	**81.6**
	2nd	82	43	3	40	**48.8**	37	**92.5**	37	**92.5**

702 † # Escapes (%) = number and percentage of regenerated plants without transgene (T-DNA) = (#Escapes/# Regenerant) X 100
703 ‡ + indicates plants PCR-positive for *hph*
704 § Transformation frequency (%) = (+ for *hph* divided by # IEs used) x 100
705 ¶ Editing efficiency (%) = (# edited plants divided by number of plants + for hph) x 100
706 †† # plants with knockout = number of plants with frameshift mutations and albino phenotypes
707 ‡‡ Knockout efficiency(%) = (# plants with knockout divided by plants + for hph) x 100